

Photonic crystal fiber interferometer for chemical vapor detection with high sensitivity

Joel Villatoro,¹ Mark P. Kreuzer,¹ Rajan Jha,¹ Vladimir P. Minkovich,²
Vittoria Finazzi,¹ Gonçal Badenes,¹ and Valerio Pruneri,^{1,3}

¹*ICFO –Institut de Ciències Fotoniques, Mediterranean Technology Park,
Av. del Canal Olímpic s/n 08860 Castelldefels, Barcelona, Spain.*

²*Centro de Investigaciones en Optica, A. C., Loma del Bosque 115, C. P. 37150 León Gto., Mexico.*

³*ICREA- Institució Catalana de Recerca i Estudis Avançats, 08010, Barcelona, Spain
joel.villatoro@icfo.es*

Abstract: We report an in-reflection photonic crystal fiber (PCF) interferometer which exhibits high sensitivity to different volatile organic compounds (VOCs), without the need of any permeable material. The interferometer is compact, robust, and consists of a stub of PCF spliced to standard optical fiber. In the splice the voids of the PCF are fully collapsed, thus allowing the excitation and recombination of two core modes. The device reflection spectrum exhibits sinusoidal interference pattern which shifts differently when the voids of the PCF are infiltrated with VOC molecules. The volume of voids responsible for the shift is less than 600 picoliters whereas the detectable levels are in the nanomole range.

©2009 Optical Society of America

OCIS Codes: (060.5295) Photonic crystal fibers; (060.2370) Fiber optics sensors; (120.3180) Interferometry; (280.4788) Optical sensing and sensors; (280.1545) Chemical analysis.

References and links

1. T. Ritari, J. Tuominen, H. Ludvigsen, J. C. Petersen, T. Sørensen, T. P. Hansen, and H. R. Simonsen, "Gas sensing using air-guiding photonic bandgap fibers," *Opt. Express* **12**, 4080-4087 (2004).
2. J. Henningsen, J. Hald, and J. C. Peterson, "Saturated absorption in acetylene and hydrogen cyanide in hollow-core photonic bandgap fibers," *Opt. Express* **13**, 10475-10482 (2005).
3. F. Benabid, F. Couny, J. C. Knight, T. A. Birks, and P. St. J. Russell, "Compact, stable and efficient all-fibre gas cells using hollow-core photonic crystal fibres," *Nature* **434**, 488-491 (2005).
4. R. Thapa, K. Knabe, M. Faheem, A. Naweed, O.L. Weaver, K. L. Corwin, "Saturated absorption spectroscopy of acetylene gas inside large-core photonic bandgap fiber," *Opt. Lett.* **31**, 2489-2491 (2006).
5. L.W. Kornaszewski, N. Gayraud, J.M. Stone, W.N. MacPherson, A.K. George, J.C. Knight, D.P. Hand, D.T.Reid, "Mid-infrared methane detection in a photonic bandgap fiber using a broadband optical parametric oscillator," *Opt. Express* **15**, 11219-11224 (2007).
6. A. M. Cubillas, M. Silva-Lopez, J. M. Lazaro, O. M. Conde, M. N. Petrovich, and J. M. Lopez-Higuera, "Methane detection at 1670-nm band using a hollow-core photonic bandgap fiber and a multiline algorithm," *Opt. Express* **15**, 17570-17576 (2007).
7. S. O. Konorov, A. Zheltikov, and M. Scalora, "Photonic-crystal fiber as a multifunctional optical sensor and sample collector," *Opt. Express* **13**, 3454-3459 (2005).
8. C. M. B. Cordeiro, M. A. R. Franco, G. Chesini, E. C. S. Barretto, R. Lwin, C. H. Brito Cruz, and M. C. J. Large, "Microstructured-core optical fibre for evanescent sensing applications," *Opt. Express* **14**, 13056-13066 (2006).
9. A. S. Webb, F. Poletti, D. J. Richardson, and J. K. Sahu, "Suspended-core holey fiber for evanescent-field sensing," *Opt. Eng.* **46**, 010503 (2007).
10. Y. Sun, X. Yu, N. T. Nguyen, P. Shum, and Y. C. Kwok, "Long path-length axial absorption detection in photonic crystal fiber," *Anal. Chem.* **80**, 4220-4224 (2008).
11. T. G. Euser, J. S. Y. Chen, N. J. Farrer, M. Scharer, P. J. Sadler, and P. St. J. Russell, "Quantitative broadband chemical sensing in air-suspended solid-core fibers" *J. Appl. Phys.* **103**, 103108 (2008).
12. C. M. B. Cordeiro, E. M. dos Santos, C. H. Brito Cruz, C. J. de Matos, and D. S. Ferreiri, "Lateral access to the holes of photonic crystal fibers – selective filling and sensing applications," *Opt. Express* **14**, 8403-8412 (2006).
13. F. M. Cox, R. Lwin, M. C. J. Large, and C. M. B. Cordeiro, "Opening up optical fibres," *Opt. Express* **15**, 11843-11848 (2007).

14. V. P. Minkovich, A.V. Kiryanov, A.B. Sotsky, and L.I. Sotskaya, "Large-mode-area holey fibers with a few air channels in cladding: modeling and experimental investigation of the modal properties," *J. Opt. Soc. Am. B* **21**, 1161-1169 (2004).
15. J. Villatoro, V. P. Minkovich, V. Pruneri, and G. Badenes, "Simple all-microstructured-optical-fiber interferometer built via fusion splicing," *Opt. Express* **15**, 1491-1496 (2007).
16. J. Villatoro, V. Finazzi, V. P. Minkovich, V. Pruneri, and G. Badenes, "Temperature-insensitive photonic crystal fiber interferometer for absolute strain sensing," *Appl. Phys. Lett.* **91**, 091109 (2007).
17. D. Káčik, I. Turek, I. Martinček, J. Canning, N. Issa, and K. Lyytikäinen, "Intermodal interference in a photonic crystal fibre," *Opt. Express* **12**, 3465-3470 (2004).
18. Y. Sun and X. Fan, "Analysis of ring resonators for chemical vapor sensor development," *Opt. Express* **16**, 10254-10268 (2008).
19. C. Elosua, I. R. Matias, C. Barriain, and F. J. Arregui, "Volatile organic compound optical fiber sensors: A review," *Sensors* **6**, 1440-1465 (2006).
20. T. L. Lowder, J. D. Gordon, S. M. Schultz, and R. H. Selfridge, "Volatile organic compound sensing using a surface-relief D-shaped fiber Bragg grating and a polydimethylsiloxane layer," *Opt. Lett.* **32**, 2523-2525 (2007).
21. Y. Sun, S. I. Shopova, G. Frye-Mason, and X. Fan, "Rapid chemical-vapor sensing using optofluidic ring resonators," *Opt. Lett.* **33**, 788-790 (2008).
22. J. Zhang, X. Tang, J. Dong, T. Wei, and H. Xiao, "Zeolite thin film-coated long period fiber grating sensor for measuring trace chemical," *Opt. Express* **16**, 8317-8323 (2008).
23. D. Monzón-Hernández, V. P. Minkovich, J. Villatoro, M. P. Kreuzer, and G. Badenes, "Photonic crystal fiber microtaper supporting two selective higher-order modes with high sensitivity to gas molecules," *Appl. Phys. Lett.* **93**, 081106 (2008).

1. Introduction

The holey structure of photonic crystal fibers (PCFs) has generated much interest in exploiting such fibers for the detection, sensing, or spectroscopic analysis of gases and liquids [1-11]. In PCFs a fraction of power of the guided light penetrates into the voids thus making possible the interaction and detection of gases or liquids by means of spectroscopic techniques. In addition to robustness and flexibility PCFs offer some advantages when used as gas or liquid cells. Firstly, the interaction lengths can be much longer than those achievable in conventional cells. On the other hand the sample volume required for filling the microscopic voids of a PCF or for measurements are much less than the volumes required in traditional gas cells. In the past few years researchers have addressed two different issues to carry out gas spectroscopy in PCFs or to design functional PCF sensors. The first one is the optimization of the PCF microstructure to maximize or enhance the overlap between guided light and gas while the second one is the simultaneous coupling of light and gas into the PCF. For example, in hollow core PCFs –which guide light by means of the photonic band gap effect- about 98% of the guided mode field energy can propagate in the core, therefore the interaction with the sample is direct [1-6]. As alternative to hollow core PCFs, solid-core and air-suspended core fibers which guide light by total internal reflection have been proposed for optical sensing [7-11]. In these types of fibers the interaction with the sample is via evanescent waves. The transmission bandwidth of index-guiding PCFs is broader than that of band-gap fibers but the energy of the evanescent fields is weaker, between 10 to 40% of the total energy of the guided mode field. Infiltrating gas into the PCF voids is a challenge, in many cases vacuum or pumping systems are required. Some alternatives that have been proposed for infiltrating gas or sample into the holes include perforation of the PCF in one side [12,13]. However, a controlled perforation is not simple; as a consequence the fiber may become lossy, weak, and fragile.

Here we demonstrate a scheme based on in reflection two-mode PCF interferometry in which the difficulty of coupling light and sample is significantly reduced. The interferometer consists of a stub of PCF spliced to standard optical fiber which exhibits high sensitivity to different volatile organic compounds (VOCs). In the splice the voids of the PCF are fully collapsed which allows the splitting and recombination of two core modes. The other end of the PCF is cleaved and the voids are left open. The device reflection spectrum exhibits a regular interference pattern. It was found that the position of the interference peaks shifted

differently when the voids of the PCF were infiltrated with vapors of methyl alcohol (CH_3OH), acetonitrile (CH_3CN), isopropanol ($\text{C}_3\text{H}_7\text{OH}$), or tetrahydrofuran (THF). No VOC permeable material is used to enhance these shifts. The latter is explained in terms of the VOCs refractive index that changes the effective index of the interfering modes. In addition to being compact and robust the interferometer is highly sensitive since a few hundred picomole can cause a detectable shift in the interference pattern. Moreover, for the interrogation an LED and a miniature spectrometer are sufficient. The total volume of the PCF voids responsible for changes in the detected signal is less than 600 picoliters. To our knowledge such a volume is the smallest one reported so far in fiber-based gas sensors.

2. Device fabrication and results

A stub of PCF (fabricated at the Centro de Investigaciones en Optica A. C.) was fusion spliced to standard optical fiber (Corning SMF-28) with a conventional splicing machine. The PCF consists of five rings of air holes arranged in a hexagonal pattern (see Fig. 1) and guides light by means of the total internal reflection effect [14]. The core and cladding diameters are $9.4\ \mu\text{m}$ and $125\ \mu\text{m}$, respectively. The average hole diameter is $2.25\ \mu\text{m}$ and the average hole spacing or pitch is $4.5\ \mu\text{m}$. The dimensions of our PCF simplify the aligning and splicing with the SMF-28 with a standard splicing machine. A default program for splicing single mode fibers was used to ensure repeatability of the process as well as to minimize the fabrication time. Under such splicing conditions the voids of the PCF collapse completely over a microscopic region whose total length is typically $\sim 300\ \mu\text{m}$ [15,16]. The collapsing of the PCF voids introduces overall optical losses in the 8-10 dB range. After the splicing, the PCF is cleaved with a standard cleaving machine so that the end of the PCF behaves as a mirror. On the other hand the voids of the PCF are left open which simplifies the infiltration of gas, chemical vapor, molecules, or any other sample. Figure 1 shows a micrograph of the described PCF, a drawing of the interferometer, and a diagram of the setup to interrogate it. Light from a broad band source such as a LED is launched to the interferometer through a fiber optic circulator or coupler. The reflected light from the cleaved end is fed to a high-resolution fiber Bragg grating (FBG) interrogation monitor (I-MON 512 Ibsen Photonics) controlled by a personal computer. This setup allowed the positional tracking of the interference peaks in real time, over millisecond time scales.

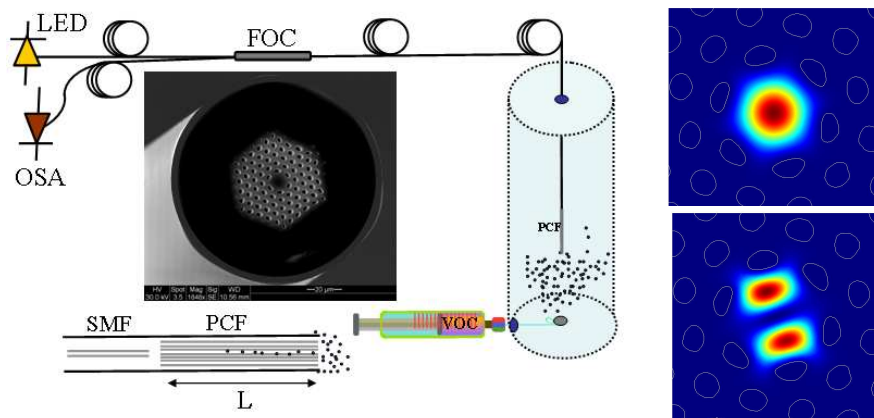


Fig. 1. (left) Diagram of the experimental setup, micrograph of the PCF used and drawing of the interferometer. L is the PCF length. LED stands for light emitting diode, FOC for fiber optic circulator or coupler, OSA for optical spectrum analyzer, and SMF for single-mode fiber. The dots represent VOC molecules. (right) Transverse component of the electric field of the LP_{01} - and LP_{11} -like modes.

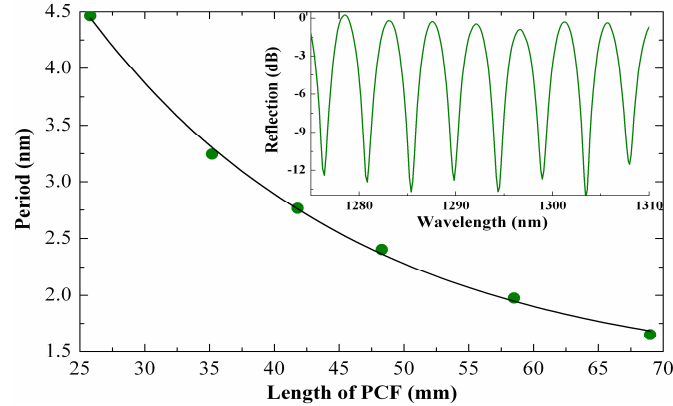


Fig. 2. Measured periods (dots) and expected ones (continuous line) as a function of length of PCF. The fringe spacing was measured in the 1275-1345 nm wavelength range. The inset shows the reflection spectrum of an interferometer fabricated with 25.8 mm of PCF.

The excitation and recombination of modes in an interferometer traditionally requires a mechanism or device that couples or excites two or more modes and one more to recombine them. Depending on the mechanism (launching or polarization conditions) or device multiple modes can be excited in the PCF [17]. In our case the excitation and recombination of modes is carried out by a single splice in which the voids of the PCF are collapsed. The fundamental SMF mode begins to diffract when it enters the collapsed section of the PCF. Because of diffraction the mode broadens allowing the excitation of two core modes in the stub of PCF [15,16]. Figure 1 shows the transverse component of the electric field of the modes that participate in the interference. The calculations were performed using finite element method (COMSOL Multiphysics) applied to the index profile based on the real PCF. The silica index was modeled using the known Sellmeier equation whereas the index of the holes was considered in the values ranging from 1 (air) to 1.1. The polymer that coats the PCF was left to absorb any cladding mode in case they are excited.

The modes propagate through the PCF until they reach the cleaved end from where they are reflected. When the reflected modes re-enter the collapsed region they are recombined in a SMF core mode. The splitting and recombination of the modes is carried out by the same splice which helps to improve the device performance. The propagation constants or equivalently the speeds of the excited modes are different; therefore they accumulate a phase difference as they propagate over the stub of fiber. Let us assume that the effective indexes of the modes are n_{e1} and n_{e2} . Thus, the accumulated phase difference is $2\pi\Delta n(2L)/\lambda$, being $\Delta n = n_{e1} - n_{e2}$, λ the wavelength of the optical source, and L the physical length of PCF, see Fig. 1. The power reflection spectrum of our interferometer will be proportional to $\cos(4\pi\Delta nL/\lambda)$. Thus, if light from a broadband source is launched to the interferometer and the reflected light fed to a spectrum analyzer, a periodic pattern can be expected. Figure 2 shows the reflection spectrum in the 1275-1310 nm range of a device fabricated with 25.8 mm of PCF. The figure also shows the average fringe spacing or periods of some fabricated interferometers as a function of the length of PCF. The measured periods agree well with the expected ones for a two-mode interferometer which is given by the expression $P \approx \lambda^2/(2\Delta nL)$. The wavelengths at which the reflection spectrum shows maxima are those that satisfy the condition $4\pi\Delta nL/\lambda = 2m\pi$, with m an integer. This means periodic constructive interference happens when $\lambda_m = (2\Delta nL/m)$.

Note that if by some means Δn changes (keeping L fixed) the position of each interference peak will change. The m -peak will shift by $\Delta\lambda_m$, the $m+1$ -peak by $\Delta\lambda_{m+1}$, and so on. This

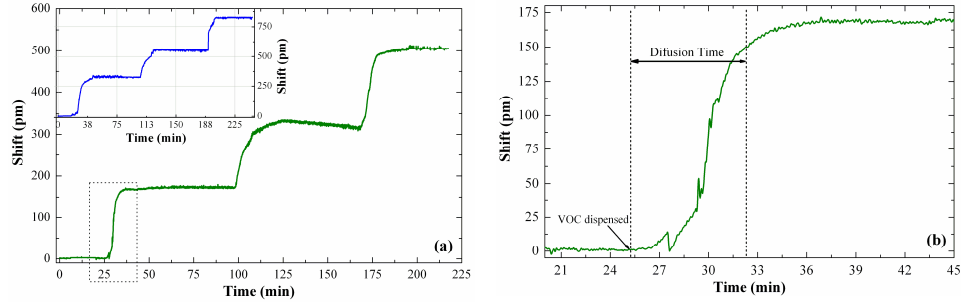


Fig. 3. (a) Shift of the interference pattern as a function time observed in a device fabricated with 22 mm of PCF when exposed to different volumes of acetonitrile and tetrahydrofuran (inset). (b) Enlarged area highlighted in (a) for acetonitrile showing both the injection and diffusion time. The light source was an LED with peak emission at 1300 nm.

means that the whole interference pattern will shift. Real time monitoring of the position of each interference maximum is straightforward. By assuming that M interference peaks are monitored simultaneously in a determined wavelength range, then the average shift (S_{av}) of the interference pattern in such a wavelength range can be defined as:

$$S_{av} = \frac{1}{M} (\Delta\lambda_m + \Delta\lambda_{m+1} + \Delta\lambda_{m+2} + \dots + \Delta\lambda_{m+M}). \quad (1)$$

Interferometers are extremely sensitive to phase changes. In our device a minute change in Δn can displace the interference pattern. The modes in our interferometer can be perturbed via evanescent waves which reach only the ring of holes adjacent to the core, see Fig. 1. Our calculations show that ~99% of the field of the LP_{01} mode and ~97% of the LP_{11} mode are in the first ring of holes of the PCF when it is filled with air. These values do not change significantly for indexes in the 1.001-1.1 range (index of some gases). However, Δn does change and cause a detectable shift in the interference pattern. This means that our interferometer can detect the presence of some gases, chemical vapor or molecules if they are present in the first ring. The total volume of such ring was calculated based on SEM images of the PCF. This ring has six holes, each hole with a diameter of ~2.25 μm . Thus, when $L = 22$ mm the volume is ~520 picoliters. Such a volume is extremely small.

Infiltrating gas or chemical vapor in the voids of the PCF interferometer and simultaneously launching light to it is not an issue in the proposed device. To this end the PCF interferometers were kept straight and secured in an enclosed container, see Fig. 1. Then they were exposed separately to different VOCs molecules by evaporating different volumes of VOC at room temperature inside the container. The VOCs were dispensed with a programmable syringe pump (Aladdin 1000, World Precision Instruments) that allowed exact control of sample quantities. The position of the interferometer and that of the syringe tip did not change during the measurements. The exposure of the interferometers to different VOC vapors shifted differently the interference patterns. Figure 3(a) for example shows the average shift of an interferometer in which L was 22 mm when exposed to vapor of acetonitrile. The inset of Fig. 3a shows the shift observed when the same interferometer was exposed to vapor of THF. These data were collected separately by firstly dispensing 5 μl of compound until it was totally evaporated. Once a steady state was attained, we added 10 more μl until it evaporated completely and measured the response. Finally we dispensed a further 20 μl and recorded the trace. Thus the total volume evaporated was 35 μl . During the first 15-25 minutes no changes are seen because we started tracking the position of the interference peaks before dispensing the VOCs in the chamber. After that time the shift increases slowly and reaches, in general, a

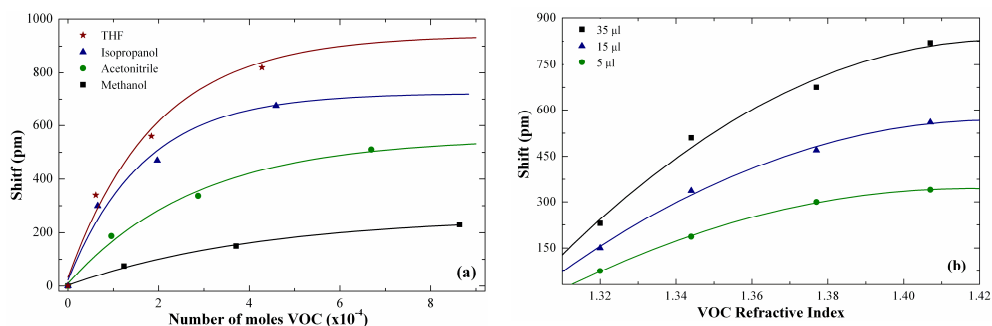


Fig. 4. (a) Average shift of the interference pattern as a function of volume of VOCs observed in a device fabricated with 22 mm of PCF. (b) Average shift as a function of the VOCs refractive index in liquid state. In both plots the symbols are experimental data and the continuous lines are fitting to the data.

steady state. Such behavior is observed in each volume evaporated. The shift increases with the evaporated volume of VOC since more molecules are present in the chamber and therefore the probability of infiltrating more molecules in the PCF voids increases. The fact that the curve plateaus indicates that the chamber was properly sealed and in this case we used excessive steady state times highlighting the stability of interferometer. No further fluctuations were present once initial plateau was achieved.

Figure 3(a) shows a zoom in of the graph obtained for acetonitrile around the minute 25. The region inside the vertical dotted lines indicates the time in which the VOC was dispensed and that in which 90% of shift was reached. Response time (the time required for a device to reach 90% of signal change) in the 5-8 minute range were calculated in our devices. Such long response times are a consequence of fact that the experiments were carried at normal conditions. Approximately between 1 and 2 minutes were needed to evaporate completed the volume of liquid dispensed in the chamber since the boiling points of the studied VOC were in the 65-83 °C. In addition, the infiltration of the VOC vapor or gas into the microscopic voids of the PCF is a diffusion process which is typically slow [1-10]. The direct introduction of gaseous samples along with smaller chamber dead volumes could lead to increased response times.

Similar plots to those shown in Fig. 3(a) were obtained when the interferometer was exposed to vapors of isopropanol and methyl alcohol (methanol). The experimental conditions were identical as in the acetonitrile and THF case. The measured shifts as a function of the number of moles and the VOC refractive index in liquid state are given, respectively, in Fig. 4(a) and 4(b). From Fig. 4(a) it can be noted that, after a certain value, dispensing more compound into the chamber (increasing the number of moles) would not lead to more appreciable shifts. The signal plateau owing to the limited volume of the PCF voids which can only house a certain number of molecules. From Fig. 4(b) one can appreciate the high sensitivity with respect to the VOCs refractive index (RI) in the liquid phase. As an average there is a ~ 4 fold increase in signal from methanol (RI of 1.320) to THF (RI of 1.407) for each volume evaporated. It can be concluded that the sensing mechanism leading to a wavelength shift of the interference pattern is due to refractive index change associated to the evaporated molecules which fill the inner holes of the PCF structure.

The detection limits of our device can be estimated if we associate the maximum shifts observed with the number of moles that the 6 holes and thus of the ~ 520 picoliter volume can house. For example, with THF the amount of VOC detected in this low volume corresponds to 6.2×10^{-7} grams or 8.6×10^{-9} moles. The corresponding values for other volumes or for other VOCs can be straightforwardly calculated by knowing their respective densities. The limits of detection of a sensor are determined by the minimal detectable shift and the sensitivity [18]. In sensing devices based on interference or resonance principles the minimum detectable shift

has to do with the width (FWHM) of the fringes or resonance peaks [18]. For the case of nanometer-width interference fringes that limit can be taken as $\sim\text{FWHM}/100$. In our 22 mm-long interferometer the FWHM of the interference fringes is ~ 4 nm which suggests that a shift of approximately 40 pm can be resolved. Although the FBG interrogator used in the experiments has a resolution of 10 pm. Therefore the limit of detection for THF lies in the $\sim 4 \times 10^{-10}$ mole range. For acetonitrile this value is $\sim 10.5 \times 10^{-10}$ moles. So basically we are capable of detecting in the few hundred or thousand picomole (10^{-12}) range for these VOCs. This is a remarkable limit of detection considering that no VOC permeable material is used. We believe these detection limits are possible thanks to the small volume of the voids responsible for the signal and for the fact that light interacts twice with the vapor.

Finally, we would like to point out that the detection of VOCs is important in a number of fields including industrial, medical, or security applications [19]. Many types of VOCs are released by paints, cleaning products, food, beverages, explosives, or even by the breath we exhale. There is a growing interest in optical methods for the detection of diverse VOCs [19-23]. Traditionally a material permeable to the target VOC is required to carry out the detection [19-23]. Photonic crystal fiber interferometers may open up new possibilities for the direct detection of VOCs as demonstrated recently by some of the present authors [23].

3. Conclusions

A photonic crystal fiber interferometer that operates in reflection was presented and its potential applications for trace chemical or gas detection demonstrated. The fabrication of the device is simple since it only involves cleaving and splicing. A microscopic collapsed region in the PCF is the key element for exciting and recombining two core modes. The interferometers exhibit regular interference patterns which shift remarkably when the voids of the fiber are infiltrated with molecules of volatile compounds. Although the volume of sample required for measurements is on the order of microliters the overall volume of voids responsible for the shifts was ~ 520 picoliters. As a consequence the detection limits of our interferometers are in the picomole range which is remarkable considering the simplicity of the device, interrogation system, and the fact that no VOC permeable material is used.

Acknowledgments

This work was carried out with the financial support of the Spanish MEC through grant TEC2006-10665/MIC and the "Ramón y Cajal" program and European Commission through the European Network of Excellence PHOREMOST (FP6-511616). The authors are grateful to S. Benchabane for her help.